Blocking Neuropilin-2 Function Inhibits Tumor Cell Metastasis

Maresa Caunt,[1,7] Judy Mak,[1,7] Wei-Ching Liang,[2] Scott Stawicki,[2] Qi Pan,[1] Raymond K. Tong,[3] Joe Kowalski,[1] Calvin Ho,[1] Hani Bou Reslan,[1] Jed Ross,[1] Leanne Berry,[1] Ian Kasman,[1] Constance Zlot,[1] Zhiyong Cheng,[1] Jennifer Le Couter,[1] Ellen H. Filvaroff,[4] Greg Plowman,[1] Franklin Peale,[5] Dorothy French,[5] Richard Carano,[1] Alexander W. Koch,[3] Yan Wu,[2,*] Ryan J. Watts,[1] Marc Tessier-Lavigne,[6] and Anil Bagri[1,*]

[1]Tumor Biology and Angiogenesis
[2]Antibody Engineering
[3]Protein Chemistry
[4]Molecular Biology
[5]Pathology
[6]Research Drug Discovery
Genentech, Inc., South San Francisco, CA 94080, USA
[7]These authors contributed equally to this work.
*Correspondence: yw@gene.com (Y.W.), abagri@gene.com (A.B.)
DOI 10.1016/j.ccr.2008.01.029

SUMMARY

Metastasis, which commonly uses lymphatics, accounts for much of the mortality associated with cancer. The vascular endothelial growth factor (VEGF)-C coreceptor, neuropilin-2 (Nrp2), modulates but is not necessary for developmental lymphangiogenesis, and its significance for metastasis is unknown. An antibody to Nrp2 that blocks VEGFC binding disrupts VEGFC-induced lymphatic endothelial cell migration, but not proliferation, in part independently of VEGF receptor activation. It does not affect established lymphatics in normal adult mice but reduces tumoral lymphangiogenesis and, importantly, functional lymphatics associated with tumors. It also reduces metastasis to sentinel lymph nodes and distant organs, apparently by delaying the departure of tumor cells from the primary tumor. Our results demonstrate that Nrp2, which was originally identified as an axon-guidance receptor, is an attractive target for modulating metastasis.

INTRODUCTION

Metastases are responsible for the majority (∼90%) of deaths associated with solid tumors (Gupta and Massague, 2006). The complex process of metastasis involves a series of distinct steps, including intravasation of tumor cells into lymphatic or blood vessels. Analysis of regional lymph nodes in many tumor types suggests that the lymphatic vasculature is an important route for the dissemination of human cancers. Furthermore, in almost all carcinomas, the presence of tumor cells in lymph nodes is the most important adverse prognostic factor. Although it was previously thought that such metastases exclusively involved passage of malignant cells along pre-existing peritumoral lymphatic vessels, recent experimental studies and clinicopathological reports (reviewed in Achen et al., 2006; Achen and Stacker, 2006; Nathanson, 2003) suggest that lymphangiogenesis induced by solid tumors can promote tumor spread. However, the role of lymphatics in association with tumors is still the subject of significant debate. Regardless, numerous recent studies suggest that targeting lymphatics and lymphangiogenesis may be a useful therapeutic strategy to restrict cancer metastasis, which would have a significant benefit for patients.

VEGFC, a member of the vascular endothelial growth factor (VEGF) family, is one of the best-studied mediators of lymphatic development. Overexpression of VEGFC in tumor cells has been shown to promote tumor-associated lymphangiogenesis,

SIGNIFICANCE

Tumor cell metastasis accounts for much of the mortality associated with cancer. Currently, there is no clinical therapeutic strategy that specifically targets the development of metastasis. Modulation of the VEGFC axis by inhibition of ligand (VEGFC) or receptor (VEGFR3) has shown promise in reducing the development of metastasis in preclinical models. We have generated a monoclonal function-blocking antibody to neuropilin-2 (Nrp2), a VEGFC coreceptor. Here, we show that anti-Nrp2 treatment inhibits the formation of functional lymphatics within tumors and inhibits the development of metastasis, in part independently of VEGF receptor activation. These data imply that Nrp2 is an attractive target for modulating metastasis.

resulting in enhanced metastasis to regional lymph nodes (reviewed in Stacker et al., 2002a, 2002b). VEGFC expression has also been correlated with tumor-associated lymphangiogenesis and lymph node metastasis for a number of human cancers (reviewed in Achen et al., 2006). In addition, blockade of VEGFC-mediated signaling has been shown to suppress tumor lymphangiogenesis and lymph node metastases in mice (Chen et al., 2005; He et al., 2002; Lin et al., 2005).

VEGFC is known to bind at least two receptor families, the tyrosine kinase VEGF receptors and the neuropilin (Nrp) receptors. VEGFC can bind VEGFR2 and VEGFR3, leading to receptor activation and autophosphorylation, which, in turn, induces angiogenesis and lymphangiogenesis (Ferrara et al., 2003). VEGFC also binds to neuropilin-2 (Nrp2) (Favier et al., 2006; Soker et al., 2002). Homozygous Nrp2 mutants show a reduction of small lymphatic vessels and capillaries prenatally (Yuan et al., 2002). These genetic studies demonstrate that Nrp2 modulates, but is not necessary for, developmental lymphangiogenesis. This raises the intriguing possibility that Nrp2 may be a modulator of tumor lymphangiogenesis and that blocking Nrp2 function may reduce metastasis, which is yet to be addressed.

Nrp2 was initially identified as a semaphorin receptor and mediator of axon guidance (Chen et al., 1997). Interestingly, many proteins that were originally discovered to be required for axon guidance during nervous system development have also been recently implicated in vascular system development (Carmeliet and Tessier-Lavigne, 2005). These observations have primarily been made for blood vessel development but are starting to extend to lymphatic vessel development as well (Yuan et al., 2002). The Nrps are one such family of axon guidance molecules that are implicated in both blood and lymphatic vessel development. Nrps have short intracellular domains that are not known to have any enzymatic or signaling activity. It has been proposed that Nrps function to enhance VEGF receptor signaling by enhancing ligand-VEGF receptor binding (Favier et al., 2006; Soker et al., 2002). In addition, Sema3F, the semaphorin ligand of Nrp2, has been shown to modulate endothelial cell behavior in vitro and in vivo (Favier et al., 2006). However, recent reports have suggested an alternate possibility that Nrps may function independently of VEGF receptors or semaphorin function to modulate endothelial cell (EC) migration (Pan et al., 2007; Wang et al., 2003).

To evaluate these mechanisms and to determine the role of Nrp2 in modulating adult lymphangiogenesis and metastasis, we generated a function-blocking antibody to Nrp2. Our in vitro analysis with this antibody suggests that Nrp2 plays a role in modulating lymphatic endothelial cell (LEC) migration and that its function extends beyond its previously assigned role as an enhancer of VEGF receptor activation. In addition, we demonstrate that blocking of Nrp2 leads to an inhibition of tumor lymphangiogenesis in adult mice. We furthermore demonstrate that treatment with anti-Nrp2 antibody results in a reduction of functional lymphatics associated with tumors. It also causes a reduction in metastasis to sentinel lymph node (SLN) and distant organs, likely by causing a delay in the efflux of tumor cells from the primary tumor. Thus, we provide strong evidence directly demonstrating the role of Nrp2, an axon guidance receptor, in modulating metastasis.
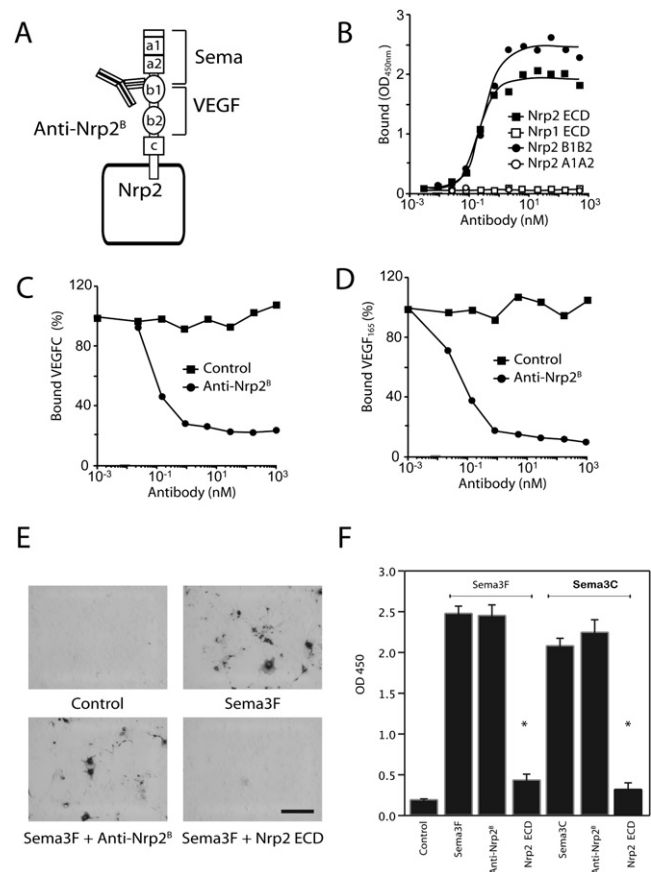

Figure 1. Characterization of Anti-Nrp2[B] mAb

(A) Schematic representation of Sema- and VEGF-binding regions on Nrp2 relative to anti-Nrp2[B] epitope regions.

(B) ELISA assay demonstrating binding of anti-Nrp2[B] to hNrp2 ECD (filled squares) and b1-b2 domains of hNrp2 (filled circles), but not hNrp1 ECD (open squares) or the a1-a2 domains of hNrp2 (open circles).

(C) Blocking of VEGFC binding to Nrp2 by anti-Nrp2[B].

(D) Blocking of VEGF binding to Nrp2 by anti-Nrp2[B].

(E) Blocking of Sema3F binding to Nrp2-293 cells. No binding was observed with alkaline phosphatase (AP) (top-left panel), but was seen with Sema3F (top-right panel). This was not blocked by anti-Nrp2[B] (bottom-left panel), but was blocked by Nrp2 ECD (bottom-right panel).

(F) Quantification of AP activity from cellular binding assay with Sema3F and Sema3C.

*$p < 0.05$; error bars represent SEM. Scale bar, 100 μm.

RESULTS

Generation of a Phage-Derived Anti-Nrp2-Specific Antibody

To evaluate the role of Nrp2 in modulating VEGFC-mediated functions, we generated a high-affinity, phage-derived monoclonal antibody (mAb) to Nrp2. The antibody was targeted to the coagulation V/VII factor (b1-b2) domains of Nrp2 (Figure 1A), which are required for VEGFC binding to Nrps (Karpanen et al., 2006). This mAb bound with similar affinity to murine (K_d of 4.9 nM) and human (K_d of 5.3 nM) Nrp2 but did not bind Nrp1 (Figure 1B). We confirmed that the mAb bound exclusively to the b1-b2 domains and did not bind to the CUB (a1-a2) domains of human Nrp2, which are primarily responsible for semaphorin
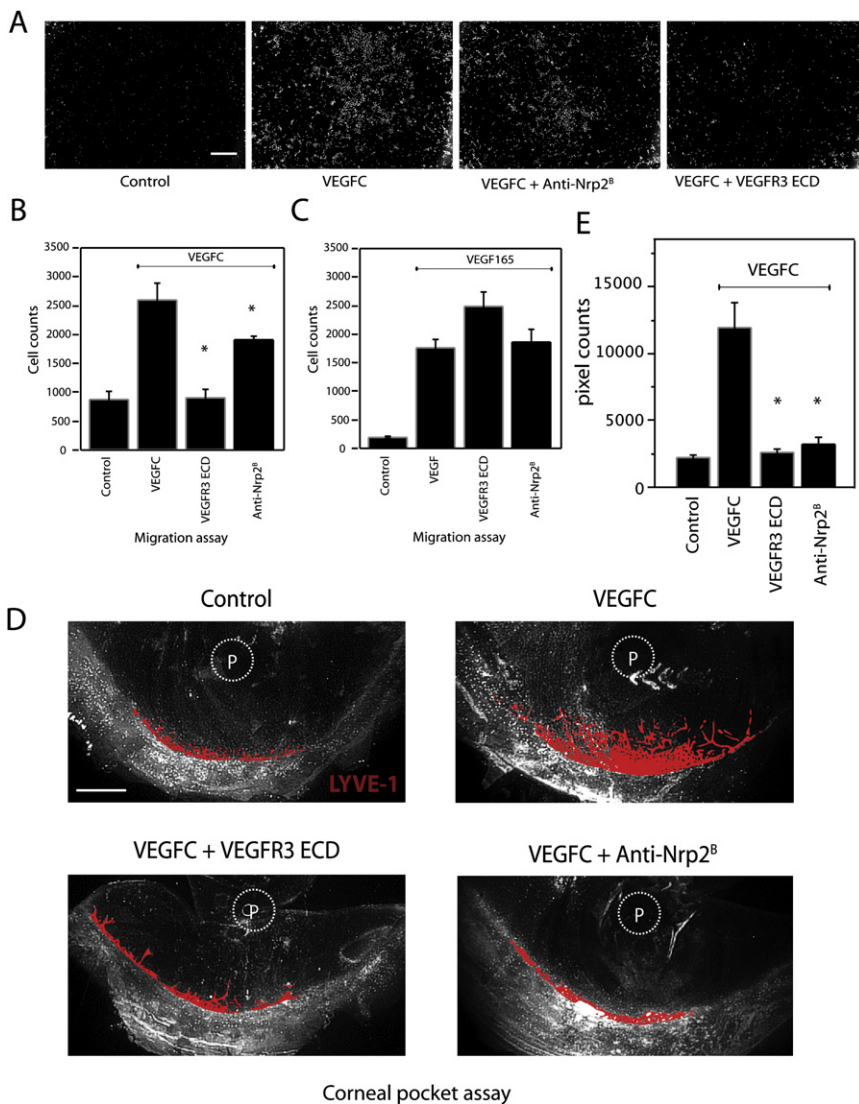
Figure 2. Anti-Nrp2[B] Reduces VEGFC-Induced Function In Vitro and In Vivo

(A) Representative images of stained LECs migrating in response to 200 ng/ml of VEGFC in the presence or absence of 50 μg/ml of anti-Nrp2[B] or VEGFR3 ECD.

(B) Quantification of LEC migration to 200 ng/ml VEGFC. For each condition, n = 6.

(C) Quantification of LEC migration to 10 ng/ml VEGF in the presence or absence of 50 μg/ml of anti-Nrp2[B] or VEGFR3 ECD. For each condition, n = 6.

(D) Representative images of LYVE-1-stained cornea, illustrating the effects of intracorneal placement of a 150 ng pellet of VEGFC (P) and systemic treatment with anti-Nrp2[B] (10 mg/kg twice weekly) or VEGFR3 ECD (25 mg/kg twice weekly). LYVE-1 staining has been pseudocolored red to facilitate visualization.

(E) Quantification of the pixel counts from the corneal micropocket assay described in (D).

$*p < 0.05$; error bars represent SEM. Scale bar, 600 μm for (A) and (D).

binding (Chen et al., 1998). Thus, we termed this mAb anti-Nrp2[B].

We then tested the ability of anti-Nrp2[B] to block binding of VEGFC or VEGF (Gluzman-Poltorak et al., 2000) to Nrp2 in both ELISA format and in cell-based binding assays. Anti-Nrp2[B] strongly blocked the binding of both VEGFC (Figure 1C) and VEGF (Figure 1D) to Nrp2 and HEK293 cells transfected with full-length Nrp2 (Nrp2-293; data not shown) with a similar IC_{50} (0.1 nM). However, anti-Nrp2[B] was not able to block binding of Sema3F or Sema3C (Chen et al., 1997) to Nrp2-293 cells (Figures 1E and 1F). These results are consistent with previous observations that the a1-a2 domains are primarily responsible for semaphorin binding and the b1-b2 domains for VEGF binding (Figure 1A).

Anti-Nrp2[B] Blocks Selective VEGFC-Mediated Functions In Vitro

We next examined the role of Nrp2 in VEGFC-mediated migration and proliferation—key cellular activities induced by VEGFC (Joukov et al., 1997). LECs have been previously shown to be

highly responsive to VEGFC (Makinen et al., 2001b). Using a transwell system, we evaluated human LEC migration to VEGFC (Figures 2A and 2B). VEGFR3 extracellular domain protein (ECD), comprising the first three (ligand binding) Ig domains of VEGFR3, was used as a positive control to block VEGFC-driven migration in this and subsequent experiments (Makinen et al., 2001a). Anti-Nrp2[B] was able to significantly reduce VEGFC-mediated LEC migration (Figures 2A and 2B; p = 0.004). The level of inhibition was lower than that seen with VEGFR3 ECD, which completely inhibited VEGFC-mediated LEC migration (Figures 2A and 2B; p = 0.002 versus anti-Nrp2[B]).

Because anti-Nrp2[B] also blocked VEGF binding to Nrp2, we evaluated the role of Nrp2 in modulating VEGF-mediated LEC migration (Makinen et al., 2001b). Anti-VEGF (B20.4.1) blocked this migration (Pan et al., 2007), whereas anti-Nrp2[B] did not have any effect (Figure 2C), possibly as a result of functional redundancy with Nrp1 (see Figure S1 available online). This hypothesis was confirmed by inhibiting Nrp1 function using anti-Nrp1[B] (Pan et al., 2007; Figures S2A and S2B). The addition of anti-Nrp2[B] to anti-Nrp1[B] did not result in any further inhibition of migration (Figures S2A and S2B), indicating that Nrp2 does not play a role in VEGF-mediated migration. Furthermore, because Nrp1 has been shown to be able to bind VEGFC (Karpanen et al., 2006), we also tested whether Nrp1 is necessary for VEGFC-induced migration. Treatment with anti-Nrp1 mAbs (Pan et al., 2007) did not result in any inhibition of VEGFC-induced migration (Figure S2C).

We next investigated the effect of anti-Nrp2[B] on VEGFC-induced LEC proliferation. Remarkably, anti-Nrp2[B] had no effect

on LEC proliferation, whereas VEGFR3 ECD provided a strong block (Figure S2D), which is in agreement with the results of previous reports showing that Nrp2 siRNA failed to inhibit VEGFC-induced proliferation in endothelial cells (Favier et al., 2006). Thus, Nrp2 appears to be important for VEGF-driven migration, but not proliferation.

We also tested the ability of anti-Nrp2[B] to modulate semaphorin function. We used the hippocampal growth cone collapse assay, which previously demonstrated that Nrp2 is required for the Sema3C- and Sema3F-mediated retraction (Chen et al., 1997). The addition of anti-Nrp2[B] did not have any effect on the semaphorin-induced collapse, whereas the addition of recombinant Nrp2 ECD inhibited this collapse completely (Figures S2E and S2F). This result is consistent with our previous observation that anti-Nrp2[B] does not interfere with Sema binding to Nrp2. Thus, anti-Nrp2[B] acts to block specific aspects of Nrp2 function, inhibiting a subset of VEGFC-mediated cellular responses but not those mediated by VEGF or Sema3F.

Anti-Nrp2[B] Blocks VEGFC-Mediated Lymphangiogenesis In Vivo

Having observed a significant reduction in LEC migration by blocking Nrp2 in vitro, we examined whether Nrp2 was required for VEGFC function in vivo. We studied two well-characterized VEGFC-mediated in vivo activities: adult lymphangiogenesis and vascular permeability (Cao et al., 2004; Joukov et al., 1998). To study lymphangiogenesis, we used the murine corneal micropocket assay (Kubo et al., 2002), in which a pellet of VEGFC induced robust lymphangiogenesis in the avascular cornea of an adult mouse over the course of 14 days (Figure 2D; 12,000 pixels with VEGFC treatment versus 2,284 pixels in control). Systemic administration of VEGFR3 ECD almost completely blocked VEGFC-induced lymphangiogenesis (2,671 pixels). Anti-Nrp2[B] also blocked the corneal lymphangiogenic response equivalently (3,281 pixels; p = 0.67 versus VEGFR3 ECD).

To evaluate vascular permeability, we used the Miles assay (Brkovic and Sirois, 2007). Remarkably, treatment with anti-Nrp2[B] had no effect on VEGFC-induced permeability, in contrast to the block observed with VEGFR3 ECD treatment (p = 0.038; Figure S3A), and demonstrated that, consistent with what we observed in vitro, Nrp2 appeared to be important for selective VEGFC-mediated functions in vivo.

Anti-Nrp2[B] Inhibits Nrp2/VEGF Receptor Complex Formation

The finding that anti-Nrp2[B] interferes with VEGFC actions was perhaps not surprising, because it blocks VEGFC binding to Nrp2. However, the fact that it blocks only selective functions both in vitro and in vivo was unexpected. One possible explanation for this selective activity is that anti-Nrp2[B] may generally inhibit LEC migration or adhesion. Anti-Nrp2[B] did not have any effect on migration induced by VEGF (Figure 2C) or hepatocyte growth factor (HGF) (Figure 3B), indicating no general disruption to LEC migration. Furthermore, anti-Nrp2[B] did not have any effect on LEC adhesion to extracellular matrix substrates fibronectin or collagen (data not shown).

A second possibility is that the anti-Nrp2[B] mAb may cause internalization of Nrp2. As Nrp2 forms a complex with VEGFR3, even in the absence of ligand (Favier et al., 2006), this could result in cointernalization of VEGFR3, affecting specific VEGFC-mediated functions. To address this possibility, we preincubated LECs with anti-Nrp2[B] at 37°C and then evaluated the level of VEGF receptors and Nrp receptors on the cell surface by FACS. No difference was observed between treatments, suggesting that anti-Nrp2[B] did not cause significant internalization of Nrp2, VEGFR2, or VEGFR3 (Figure 3A). Because VEGFC can potentiate the interaction between Nrp2 and VEGF receptors, we conducted similar internalization experiments in the presence of 200 ng/ml of VEGFC. Again, no difference was observed between treatments (Figure S3E).

Because Nrp2 has been proposed to augment VEGF receptor signaling (Favier et al., 2006), we next studied the effect of anti-Nrp2[B] on VEGFR2 and VEGFR3 activation, in which VEGFC stimulation leads to receptor dimerization and autophosphorylation. VEGFR3 ECD completely blocked VEGFC-mediated VEGFR2 (Figure S3B) and VEGFR3 (Figure 3C) phosphorylation. Anti-Nrp2[B] treatment resulted in a reduction of VEGFR2 (Figure S3B) and VEGFR3 (Figure 3C) activation, but to a lesser degree than VEGFR3 ECD treatment. This observation raised the possibility that the selective inhibitory activity of anti-Nrp2[B] could be a result of differential requirements of VEGF receptor activation for migration and proliferation. To address this possibility, we evaluated the dose response of VEGFR2 and VEGFR3 phosphorylation to VEGFC stimulation (Figure 3C and Figure S3B). We consistently observed that the reduction by anti-Nrp2[B] treatment of VEGFR2 phosphorylation stimulated by 200 ng/ml of VEGFC was roughly equivalent to the VEGFR2 phosphorylation obtained by stimulating with 175 ng/ml or 150 ng/ml of VEGFC in the absence of antibody. This result was also noted to be the case for VEGFR3. We then performed a dose-response analysis of migration to VEGFC stimulation. We reasoned that, if the reduction in VEGF receptor activation alone was responsible for the reduced migration seen with anti-Nrp2[B] treatment, then stimulation of LECs with 150 or 175 ng/ml of VEGFC should have similar reduced degree of migration as well. However, we did not see any reduction of LEC migration with 175 or 150 ng/ml of VEGFC (Figure 3D). A significant reduction in migration was not observed until VEGFC levels were reduced to 50 ng/ml. We therefore reasoned that the reduction in VEGF receptor activation induced by anti-Nrp2[B] was, by itself, insufficient to reduce migration. We also evaluated the effect of anti-Nrp2[B] on downstream signaling events mediated by VEGF receptors. Treatment with anti-Nrp2[B] or stimulation with 150 ng/ml of VEGFC did not significantly reduce activation of Erk1/2 or p38 MAPK (Figure S3D), which modulate VEGF receptor-mediated proliferation and motility, respectively. This result indicated that Nrp2 might regulate LEC migration and lymphangiogenesis by a mechanism other than enhancing VEGF receptor activation or downstream signaling.

Finally, we tested the effect of anti-Nrp2[B] on Nrp2/VEGF receptor complex formation. As reported elsewhere, Nrp2 can be coimmunoprecipitated with VEGFR2 and VEGFR3 in the presence or absence of VEGFC (Favier et al., 2006; Karpanen et al., 2006), and this interaction was dramatically reduced by anti-Nrp2[B] (Figure 3E and Figure S3C). This result suggests that the Nrp2/VEGF receptor complex is important for specific VEGFC-mediated functions. Furthermore, the role of Nrp2 is
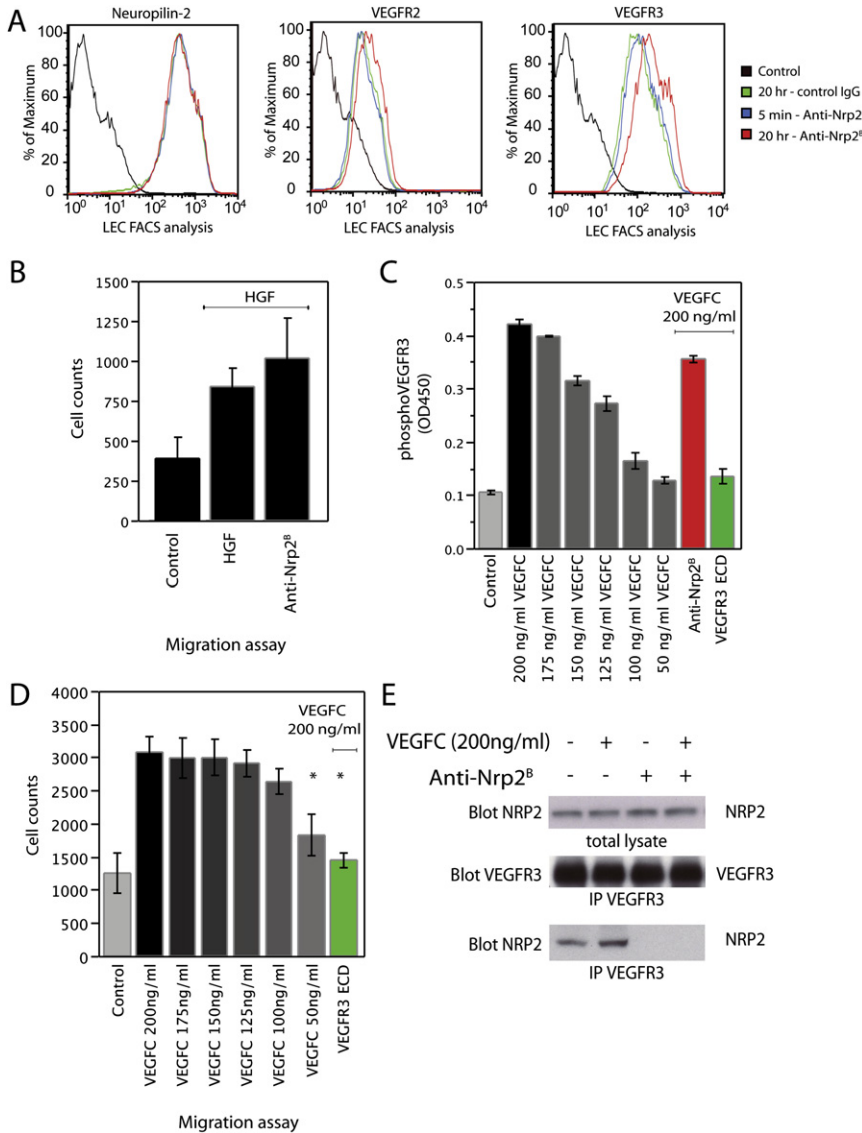
Figure 3. Nrp2[B] Treatment Results in a Reduction in VEGF Receptor Activation and Inhibits Nrp2/VEGF Receptor Complex Formation

(A) FACS analysis of Nrp2, VEGFR2, and VEGFR3 levels on the surface of LEC after treatment with control antibody (10 μg/ml; green line) or anti-Nrp2[B] (10 μg/ml) for 5 min (blue line), or 20 hr (red line).

(B) Quantification of LEC migration to 20 ng/ml HGF in the presence or absence of 50 μg/ml of anti-Nrp2[B] or VEGFR3 ECD. For each condition, n = 6.

(C) VEGFR3 phosphorylation level as assayed by the VEGFR3 KIRA assay. pVEGFR3 levels in anti-Nrp2[B] (10 μg/ml)-treated cells was significantly different from the VEGFC stimulation at 200 ng/ml and consistently lay between the phosphorylation level induced by 175 ng/ml and 150 ng/ml of VEGFC. For each condition, n = 6.

(D) Quantification of LEC migration to VEGFC (concentration as noted) in the presence or absence of VEGFR3 ECD (10 μg/ml). Significant reductions in migration were noted at 50 ng/ml of VEGFC or when blocked with VEGFR3 ECD.

(E) Immunoprecipitation with anti-VEGFR3. Cell lysate or immunoprecipitation (IP) material was probed with anti-Nrp2 or anti-VEGFR3 as indicated.

*p < 0.05; error bars represent the SEM. Each experiment was repeated a minimum of three times.

expression was confirmed by ISH in a subset of tumor types (Figure S4B). These tumor-associated lymphatic vessels are likely a result of active lymphangiogenesis (Achen et al., 2006). To evaluate Nrp2 expression in newly growing vessels, we stained corneas from the corneal micropocket assay described above. We saw Nrp2 expression in new lymphatics vessels (Figure 4F), with stronger expression seen in the growing tip of the vessel. Thus, Nrp2 is not expressed in quiescent adult lymphatics but is present during lymphangiogenesis, in both development and adult tissues.

Anti-Nrp2[B] Reduces Lung Metastasis in Multiple Tumor Models

One major approach to studying metastasis has been via inhibition of the VEGFC axis in orthotopic (Chen et al., 2005) or heterotopic subcutaneous (He et al., 2002; Krishnan et al., 2003; Lin et al., 2005) tumor models. To determine whether blocking Nrp2 function could also modulate the development of metastasis, we tested the effects of anti-Nrp2[B] treatment on the formation of lung metastasis in two different tumor models—66c14 and C6 tumor models. We evaluated distant organ metastasis, because it represents the end result of the metastatic cascade and allows us to determine whether inhibition of Nrp2 has a meaningful role in reducing metastasis. 66c14 is a murine mammary carcinoma line derived from a spontaneous tumor; it expresses VEGFC and metastasizes via the lymphatic system to

not exclusively to enhance VEGF receptor signaling in response to ligand stimulation.

Nrp2 Is Expressed in Tumor-Associated Lymphatics

As reported elsewhere (Yuan et al., 2002), Nrp2 staining is present in developing lymphatic vessels found in E12.5 mice (Figure 4A). To determine whether Nrp2 plays a role in adult lymphatic biology, we evaluated the expression of Nrp2 in adult lymphatics. As described above, LECs in culture strongly express Nrp2 (Figure S1). However, we were unable to detect Nrp2 by immunohistochemistry (IHC) in LYVE-1-positive lymphatic vessels of colon or lymph node in normal adult mice (Figures 4B and 4C), confirmed by Nrp2 in situ hybridization (ISH; Figure S4C). In contrast, strong Nrp2 expression was observed in LYVE-1-positive lymphatic vessels, within and around tumors and in lymph nodes adjacent to tumors (Figure 4D). This was observed with a number of tumor lines, including the breast adenocarcinoma line (66c14) (Aslakson and Miller, 1992), the rodent glioblastoma line (C6), and human prostate carcinoma (PC3 line) (Figure 4E). This
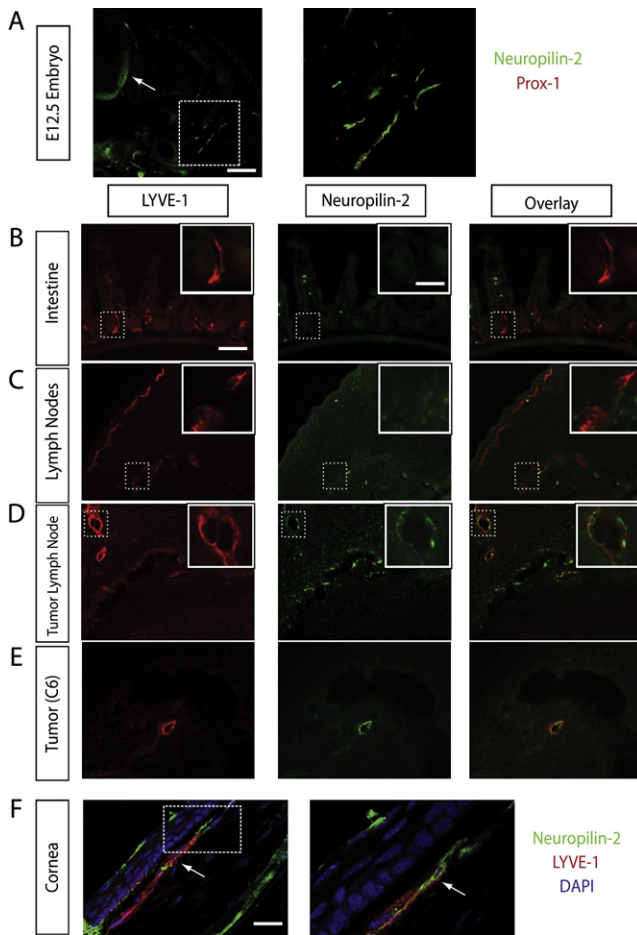
Figure 4. Nrp2 Is Expressed Developmentally and in the Lymphatics of Tumor-Bearing Mice

(A) Nrp2 staining (green) in E12.5 mouse embryo sections colocalizes with Prox-1 (red) staining lymphatic endothelial cells. Additionally, Nrp2-stained axons can be seen in the spinal cord (arrow), in the expected pattern acting as a positive control for Nrp2 IHC. A higher magnification of the boxed area is shown in the right panel.

(B and C) LYVE-1 staining (left column, red) labeling lymphatics, Nrp2 staining (middle column, green), and the overlay (right column) in the (B) intestine and (C) lymph node of normal adult mouse. Nrp2 signal does not colocalize with LYVE-1-labeled lymphatics in either organ.

(D) In lymph nodes from tumor-bearing animals, Nrp2 signal does colocalize with LYVE-1-positive lymphatic vessels lining the LN sinuses.

(E) Strong Nrp2 staining is also seen in lymphatic vessels within C6 tumors. Boxed areas are shown at high magnification within insets.

(F) Nrp2 and LYVE-1 double staining in a cross-section of cornea from a corneal micropocket assay. The specimen is oriented so that the VEGFC pellet was placed above the upper border of the image. An LYVE-1-positive (red) vessel (arrow) can be seen to express Nrp2 (green). Nrp2 can also be seen in Descement's membrane and in cells of the anterior corneal epithelium. More Nrp2 staining is seen in the growing tip of the vessel. A higher magnification of the boxed area is shown in the right panel and shows Nrp2 staining in the growing vessel tip.

Scale bar, 200 μm for (A)–(E) (60 μm for inserts) and 100 μm for (F).

the lungs (Aslakson and Miller, 1992). Anti-Nrp2[B] treatment did not affect the primary growth rate of the tumors (Figure 5A). Because VEGFR3 ECD did reduce 66c14 primary tumor growth rates (data not shown), it was excluded from any further analysis
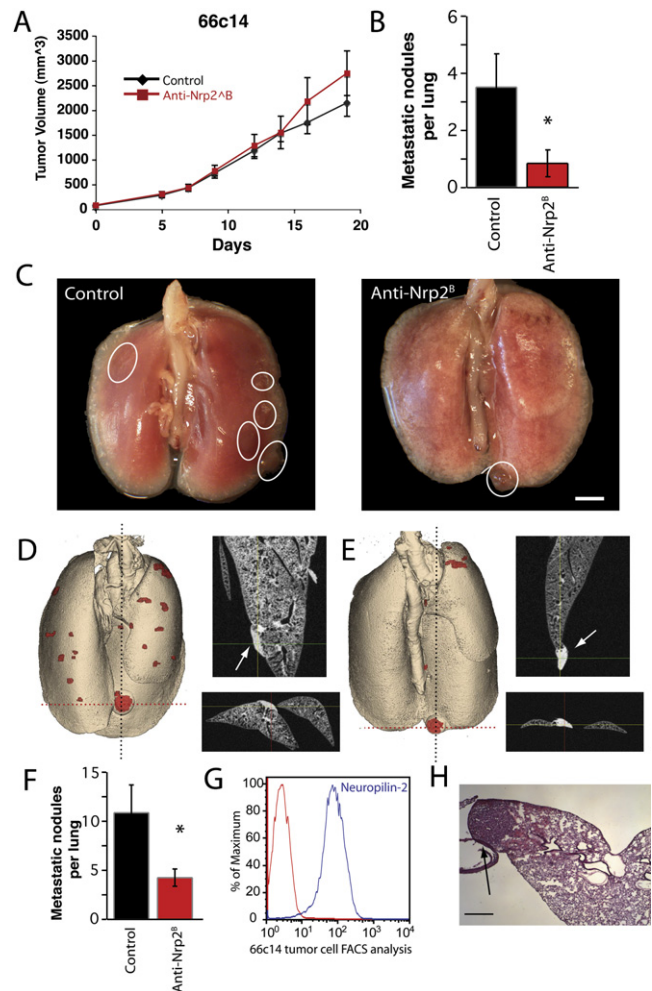

Figure 5. Anti-Nrp2[B] Treatment Results in a Reduction of Lung Metastasis in the 66c14 Tumor Model

(A) Mean tumor volume graph of 66c14 tumor model study analyzed below.

(B) Quantification by visual inspection of the number of metastatic nodules per lung in control and anti-Nrp2[B]-treated animals.

(C) Representative images of lungs from control (left) and anti-Nrp2[B]-treated (right) animals. Lungs were inflated prior to fixation by right cardiac ventricular perfusion. Nodules are highlighted in white to facilitate visualization.

(D and E) Three-dimensional renderings of representative micro-CT scanned lungs demonstrating metastatic nodules (red) in control (D) and anti-Nrp2[B]-treated (E) animals. The positions of the longitudinal section (top inset) and the cross-section (bottom insert) are indicated by the black and red dotted lines respectively.

(F) Quantification of the number of metastatic nodules per lung by micro-CT analysis of the lungs.

(G) FACS analysis of Nrp2 levels on the surface of in vitro-cultured 66c14 tumor cells.

(H) H&E staining of a lung nodule (arrow) demonstrating metastatic tumor cells.
*$p < 0.05$; error bars represent SEM. Scale bar, 2 mm for (C) and 400 μm for (H).

of metastasis. A cohort of animals (n = 6) with similar sized tumors from both arms were killed concurrently, and the lungs were harvested and evaluated for metastasis. Anti-Nrp2[B] caused a significant reduction in the average number of visually detected metastatic nodules per lung, compared with control IgG-treated animals (Figures 5B and 5C), from an average of 3.5 to 0.8

(p = 0.03). To confirm this result and extend our evaluation to lung parenchyma, we performed a micro-CT analysis (Li et al., 2006) of the lungs. This analysis confirmed that anti-Nrp2[B]-treated animals had a reduction in the number of lung metastasis, compared with control-treated animals (Figures 5D, 5E, and 5F). Micro-CT analysis was more sensitive, resulting in detection of a larger absolute number of metastatic nodules in both groups. Micro-CT also allowed us to determine the total metastatic burden within the lung. Anti-Nrp2[B] treatment also resulted in a reduction of total metastatic volume (0.74 cm^3) in comparison to control treatment (1.78 cm^3).

FACS analysis indicated that Nrp2, but not VEGFR2 or VEGFR3, was expressed on 66c14 tumor cells (Figure 5G and Figure S5). This raised the possibility that treatment with anti-Nrp2[B] was affecting tumor cell behavior directly to impact metastasis. Anti-Nrp2[B] did not have any effect on tumor cell proliferation, apoptosis, or migration in vitro (data not shown). However, to address the possibility that the reduction in metastasis was due to effects of anti-Nrp2[B] on tumor cells, we also evaluated the effect of anti-Nrp2[B] on subcutaneously transplanted C6 tumor cells. These cells do not express Nrp2 on their surface to an appreciable degree (Figure 6E), but they do express VEGFC and are thought to metastasize to the lung via the lymphatic system (Bernstein and Woodard, 1995). Additionally, they have been engineered to express β-galactosidase to facilitate detection of tumor cells.

Anti-Nrp2[B] treatment did not affect the primary growth rate of these tumors (Figure 6A). Additionally, VEGFR3 ECD did not dramatically reduce primary tumor growth rate in this tumor model, allowing for comparisons of the antimetastatic effects of VEGFR3 ECD and anti-Nrp2[B]. Again, a cohort of animals (n = 10) with similar sized tumors from all treatment arms were killed, and the lungs were assessed. Treatment with either anti-Nrp2[B] or VEGFR3 ECD caused a reduction in the average number of visually detected metastatic nodules per lung (Figures 6B and 6C). The reduction noted with anti-Nrp2[B] was comparable to that seen with VEGFR3 ECD. Micro-CT analysis of the lungs confirmed these findings (Figure 6D). Nodules were confirmed to be metastatic lesions by histology in both tumor models (Figures 5H and 6F). Additionally, general necropsy did not reveal nodules on the surface of other organs in either tumor model.

Blocking Nrp2 Function Results in a Reduction of Tumor Lymphatics

To understand the mechanism by which anti-Nrp2[B] treatment reduced metastasis, we evaluated the primary tumors (n = 5 animals per group for both studies). For 66c14 or C6 tumors, the general architecture of tumor tissue was comparable between control and anti-Nrp2[B]-treated tumors by hematoxylin and eosin (H&E) staining (data not shown). In addition, Ki67 IHC and TUNEL staining did not demonstrate any differences in proliferation or apoptosis in the tumors (data not shown), consistent with the similar growth rates observed. Because metastases are thought to occur via blood or lymphatic vessels, we also used PECAM-1 and LYVE-1 IHC, respectively, to evaluate these vessels within tumors. PECAM-1 staining revealed no morphological or quantitative differences between control and anti-Nrp2[B]-treated tumors in the 66c14 study and between control, anti-Nrp2[B]-treated, and VEGFR3 ECD-treated tumors in the C6 study (Figures 7A and 7C).
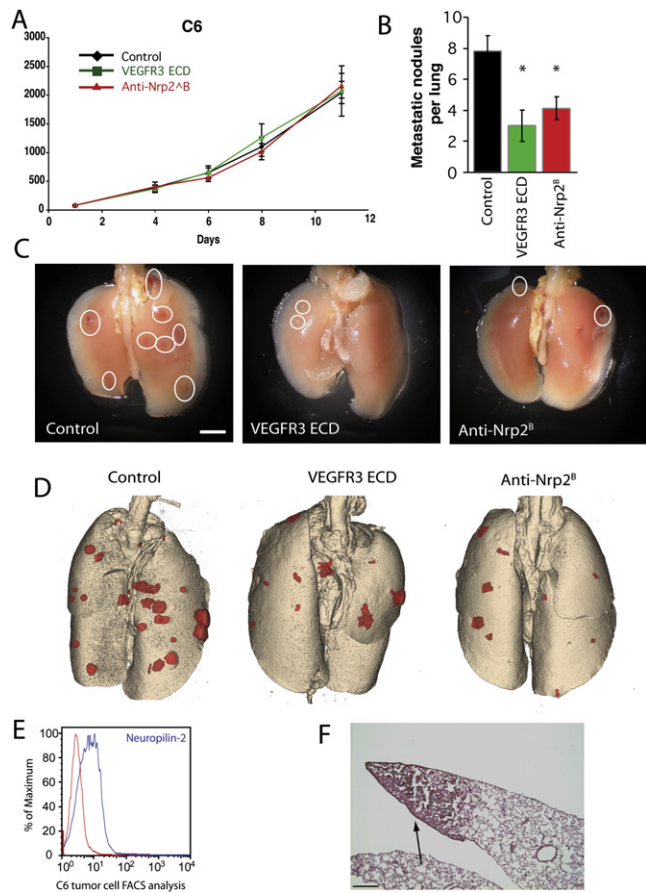

Figure 6. Anti-Nrp2[B] Treatment Results in a Reduction of Lung Metastasis in the C6 Tumor Model

(A) Mean tumor volume graph of C6 tumor model study analyzed below.

(B) Quantification by visual inspection of the number of metastatic nodules per lung in control, VEGFR3 ECD-treated, and anti-Nrp2[B]-treated animals.

(C) Representative images of lungs from control (left), VEGFR3 ECD-treated (middle), and anti-Nrp2[B]-treated (right) animals. Nodules are highlighted in white to facilitate visualization.

(D) Three-dimensional renderings of representative micro-CT scanned lungs demonstrating metastatic nodules (red) in control (left), VEGFR3 ECD-treated (middle) and Anti-Nrp2[B]-treated (right) animals.

(E) FACS analysis of Nrp2 levels on the surface of in vitro-cultured C6 tumor cells.

(F) H&E staining of a lung nodule (arrow) demonstrating metastatic tumor cells.

*p < 0.05; error bars represent SEM. Scale bar 2 mm for (C) and 400 μm for (F).

In contrast, LYVE-1 staining revealed a dramatic reduction of lymphatic vessel density in anti-Nrp2[B]-treated tumors, compared with control tumors, in both 66c14 and C6 studies (Figures 7B and 7C). Furthermore, the level of reduction was quantitatively similar to that seen with VEGFR3 ECD treatment (Figure 7C). Anti-Nrp2[B] treatment also led to differences in lymphatic morphology, compared with control tissue (Figure 7C, middle and lower panels). The lymphatic structures in control tumors formed complex networks with large luminal vessels lined by intact LECs (Ji and Kato, 2003). However, the lymphatic structures in anti-Nrp2[B]-treated tumors were rare single vessels with small lumens. More commonly, small regions of multiple isolated LECs were noted in anti-Nrp2[B]-treated tumors. Despite the similar
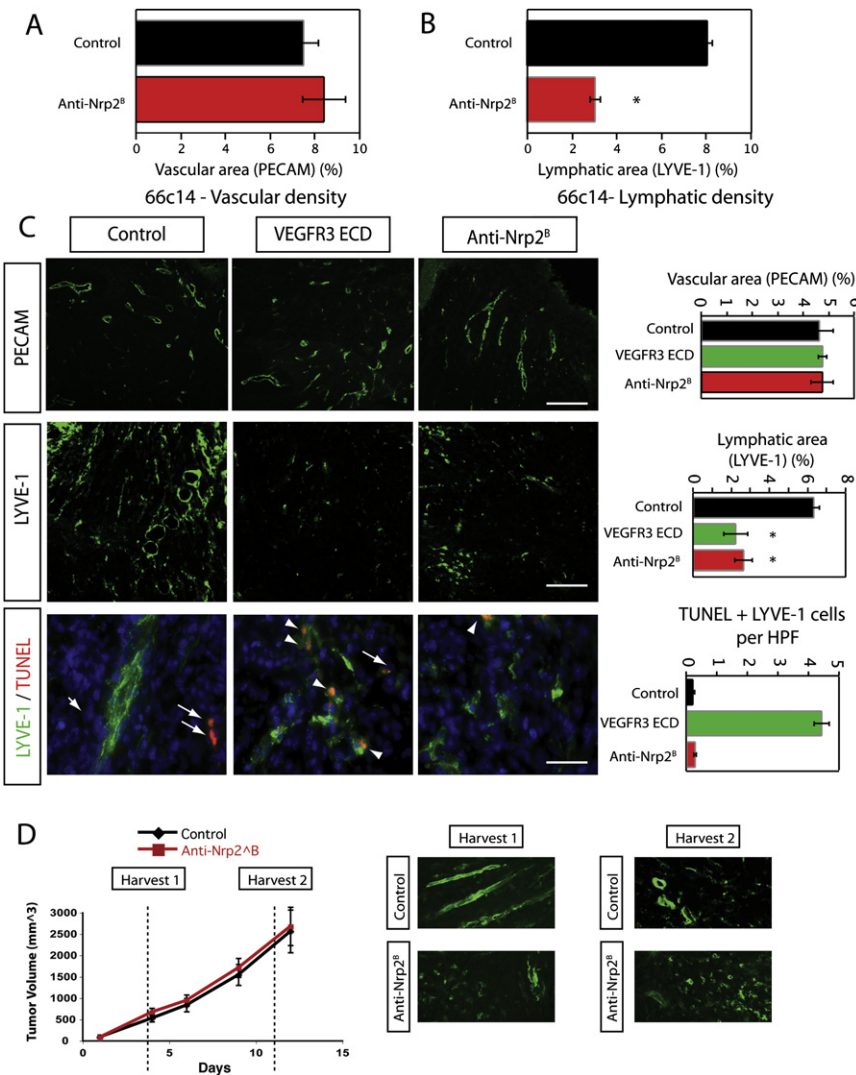
Figure 7. Anti-Nrp2[B] Treatment Results in a Reduction of Tumor Lymphatic Vessels

(A and B) Quantification of vascular vessel density (A) by PECAM-1 IHC and lymphatic vessel density (B) by LYVE-1 IHC in 66c14 tumors treated with control antibody or anti-Nrp2[B]. Vessel density was determined from 6 representative images from each of 6 tumors per group, evaluated for mean pixel number by ImageJ.

(C) Representative mages of PECAM-1 stained vessels (top row) and LYVE-1 stained lymphatic vessels (middle row) and LYVE-1/TUNEL double stained (bottom row) in C6 tumors treated with control antibody (left column), VEGFR3 ECD (middle column) or Anti-Nrp2[B] (right column). While TUNEL positive apoptotic cells (red) are present in control tissue (arrows), they are not associated with intact lymphatic vessels (green). In contrast, many LYVE-1/TUNEL double stained cells (arrow heads) are noted in the disrupted and fragmenting lymphatics of VEGFR3 ECD-treated tumors. Clusters of single lymphatic endothelial cells with rare apoptotic lymphatic cells are noted in Anti-Nrp2[B]-treated tumors. Quantification of vascular (top graph) and lymphatic (middle graph) vessel density and number of LYVE-1/TUNEL double positive cells (bottom graph) are to the right of these images. Images and quantification primarily limited to 1 mm from the edge of the tumor margin.

(D) LYVE-1 stained tumors from Anti-Nrp2[B]-treated animals (bottom panels) harvested at day 4 (Harvest 1) and day 11 (Harvest 2) demonstrate disruption of lymphatic vessels in comparison to control-treated animals (top panels). The harvest dates relative to growth curves are shown to the left.

*p < 0.05; error bars represent SEM. Scale bar, 200 μm for (C) (top, middle row) and 50 μm for (C) (bottom row) and (D).

reduction in lymphatic vascular density, the morphology of lymphatic vessels was different in VEGFR3 ECD-treated tumors, where sparse networks comprised small vessels lined by fragmenting LECs. Only rarely were intact lymphatic vessels observed. IHC with podoplanin, another marker of lymphatics, confirmed these findings (data not shown). We also conducted LYVE-1 and TUNEL double staining on these tissues to determine whether the number of apoptotic lymphatics cells was increased in response to treatment (Figure 7C). We observed a significant increase in the number of apoptotic lymphatic cells in VEGFR3 ECD-treated tumors, in comparison to control tumors. Interestingly, there was no significant increase in the number of apoptotic lymphatic cells in tumors treated with anti-Nrp2[B] (Figure 7C). We propose that the reduction of metastasis seen with anti-Nrp2[B] treatment is due to the reduction of tumor-associated lymphatics, as has been hypothesized in studies blocking VEGFC function (He et al., 2002).

Next, we sought to determine whether anti-Nrp2[B] acts by inhibiting tumor lymphangiogenesis or by disrupting existing mature tumor lymphatics. To address this issue, we evaluated tumors that were harvested from control and anti-Nrp2[B]-treated

tumors at early and late time points in the study. If at early time points, anti-Nrp2[B]-treated tumors had intact lymphatic networks, the likely mechanism for anti-Nrp2[B] action would be disruption of existing lymphatics. However, if at early time points, these tumors had abnormal lymphatics, the likely mechanism would be an inhibition of tumor lymphangiogenesis. We compared lymphatic development in treated and control tumors at both time points. Day 4 (after initiation of anti-Nrp2[B] treatment) was selected as the early time point, because it was the first time point when control-treated primary tumors had mature lymphatic vessels. We observed similar disrupted lymphatic morphologies in early and late time points in anti-Nrp2[B]-treated tissue, suggesting that anti-Nrp2[B] disrupts the formation of lymphatic structures (Figure 7D).

Finally, we evaluated the effects of anti-Nrp2[B] treatment on the normal lymphatics in adult mice. Analysis of intestinal, cutaneous, pancreatic, and lymph node lymphatics by LYVE-1 IHC of mice treated for five weeks with anti-Nrp2[B] revealed no qualitative or quantitative differences between treated and untreated mice (Figure S6). This suggests that blocking of Nrp2 does not affect maintenance of quiescent adult lymphatics.
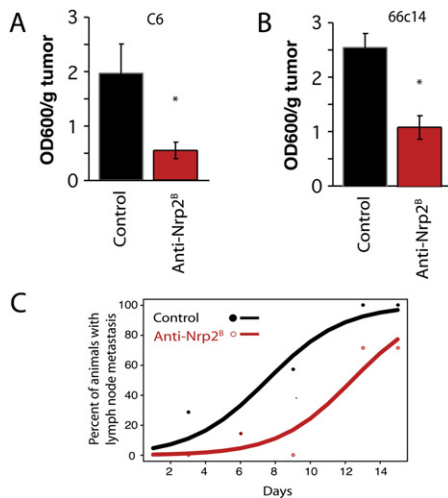
Figure 8. Anti-Nrp2[B] Treatment Results in a Reduction of Functional Tumor Lymphatic Vessels and Leads to a Delay in Metastasis to the Primary Lymph Node

(A and B) Anti-Nrp2[B] treatment results in a reduction of Evans Blue within C6 (A) ($p = 0.035$) and 66c14 (B) ($p = 0.005$) tumors, indicating a reduction in functional lymphatics within these treated tumors.

(C) Percentage of animals with SLNs containing β-gal expressing C6 tumor cells at various time points after tumor implantation in the ears of control (black) and anti-Nrp2[B]-treated (red) mice. Anti-Nrp2[B] treatment results in a delay of arrival of cells at the SLN ($p = 0.006$). n = 7 animals per treatment condition per time point.

*$p < 0.05$; error bars represent SEM.

Nrp2 Inhibition Leads to a Reduction in Functional Lymphatics

Our results demonstrate that anti-Nrp2[B] treatment reduced the lymphatic vessel density within tumors. We next tested the effects of anti-Nrp2[B] treatment on functional tumor lymphatics, because these were most likely to be involved in metastasis. We employed the commonly used technique of intradermal lymphangiography with Evans Blue (Isaka et al., 2004), because it can be easily extracted from tissue and quantified. Tumor lymphatics likely sprout from dermal lymphatics and are, therefore, continuous with them. Because the dermal lymphatics drain deeply (toward the larger lymphatic vessels in the center of the body), the dye injected intradermally, which enters the skin lymphatics, can, paradoxically, travel to the tumor on its way to the sentinel lymph node (Padera et al., 2002). Lymphangiography was performed on control and anti-Nrp2[B]-treated mice bearing C6 and 66c14 tumors between 500 and 600 mm^3 (before the onset of tumor necrosis). As Evans Blue dye was transported into the tumor primarily by lymphatic vessels, we quantified the total tumor Evans Blue content as a measure of functional lymphatics within the tumors. Nrp2[B] treatment resulted in a dramatic reduction in Evans Blue levels within tumors (0.55 OD$_{600}$/g) (Figures 8A and 8B; n = 4). We did not anticipate any nonspecific leakage, because the dye was injected into normal skin, where Evans Blue could not cross blood vessel walls. To confirm this, we also tested the blood from these animals for Evans Blue, which was not present at detectable levels. This result strongly suggests that anti-Nrp2[B] treatment results in a reduction of functional lymphatics within tumors.

Blocking Nrp2 Function Results in a Delay of Metastasis via the Lymphatic System

We predicted that blocking Nrp2 function should result in a delay of one of the early steps in the metastatic cascade—arrival of tumor cells at the sentinel lymph node (SLN). The SLN is the first tissue that metastasizing cells encounter after exiting the tumor and entering the lymphatic system. Thus, we performed a subcutaneous transplantation of C6 tumor cells into the ear, because it has a well-defined lymphatic drainage pattern and a single SLN (Hoshida et al., 2006). Animals were removed from control and anti-Nrp2[B] treatment arms at various time points, and SLNs were evaluated for the presence of metastatic cells in a highly sensitive manner (as few as 10 tumor cells could be detected; data not shown) by assessing β-galactosidase activity. Tumor cells were identified in the SLNs of control animals as early at 3 days after implantation (Figure 8C). Micrometastasis was initially identified in anti-Nrp2[B]-treated SLNs at 6 days postimplantation. As predicted, analysis of the remainder of the time course revealed a significant delay in the development of tumor cell-positive SLNs in anti-Nrp2[B]-treated animals. Furthermore, a reduction in formation of positive SLNs in addition to this observed delay cannot be ruled out.

DISCUSSION

A key early event in metastasis involves the egress of tumor cells from the primary tumor, often via the lymphatic system. VEGFC is a key modulator of lymphangiogenesis and metastasis in many tumor models, and inhibition of the VEGFC axis is considered a promising strategy for inhibiting the development of metastasis. To date, Nrp2, a coreceptor for VEGFC, has not been a target for inhibiting metastasis. Our studies support an important role of Nrp2 in tumor lymphangiogenesis and metastasis, only in part by modulating VEGFR3 signaling. In addition, we demonstrate that treating with anti-Nrp2[B] results in a reduction of functional lymphatics, impacting the early steps of metastasis to SLNs.

Nrp2 Regulates Selective VEGFC Functions, in Part through a Mechanism Independent of VEGF Receptor Activation

Induction of migration and proliferation are two key cellular functions of VEGFC (Joukov et al., 1997). Our finding that blocking Nrp2 with anti-Nrp2[B] blocked LEC migration but not proliferation (Figures 2 and 3) was therefore surprising. A similar selectivity, recently reported with Nrp2 siRNA knockdown experiments, was attributed to experimental technical limitations (Favier et al., 2006). We also demonstrated Nrp2's functional selectivity in vivo, because anti-Nrp2[B] treatment resulted in a reduction of VEGFC-driven lymphangiogenesis but not vascular permeability (Figures 2 and 3). This insensitivity of permeability to treatment with anti-Nrp2[B] may reflect the minimal biological relevance of the Nrp2-VEGFR2 interaction (permeability is primarily mediated by VEGFR2), differential sensitivity of lymphangiogenesis and vascular permeability to Nrp2 inhibition, or the fact that lymphangiogenesis requires LEC migration, whereas permeability may not. Nevertheless, these observations suggest that inhibition with anti-Nrp2[B] does not simply disrupt VEGFC signaling. Blocking of Nrp2 did result in a modest reduction in VEGF receptor phosphorylation (Figure 3), supporting a mechanism whereby

one role of Nrp2 is to enhance VEGF receptor function, consistent with previous reports (Favier et al., 2006). However, because this lower level of receptor phosphorylation was still able to maximally drive LEC migration, we determined that the observed in vitro inhibition of migration could not be exclusively attributed to this reduction in VEGF receptor phosphorylation (Figure 3). This suggested an additional role for Nrp2 in this process.

We therefore investigated other mechanisms by which blocking of Nrp2 may selectively affect migration, such as modulation of adhesion or motility. Anti-Nrp2[B] treatment did not have any effect on LEC-mediated adhesion (data not shown) or non-VEGFC-induced migration (Figures 2 and 3), indicating that this was unlikely. Sema3F, another ligand of Nrp2, may modulate LEC or EC migration, acting as a chemorepellent (Favier et al., 2006). However, our antibody did not alter the binding of Sema3F to Nrp2 (Figure 1) or the functional effects of Sema3F (Figure S2). Thus, it is unlikely that the reduction in VEGFC-induced migration by anti-Nrp2[B] is a result of modulation of Sema3F function.

We also evaluated the effect of anti-Nrp2[B] on the formation of the Nrp2/VEGF receptor complex. Nrp2 forms a complex with VEGFR2 and VEGFR3 in the absence of ligand (Favier et al., 2006; Karpanen et al., 2006), and anti-Nrp2[B] inhibits the formation of these complexes. This observation, coupled with the fact that Nrp2 is significant for more than just augmentation of VEGF receptor function, supports a model in which Nrp2 specifically modulates migration as part of the receptor complex, potentially by binding additional molecular mediators. A similar mechanism of action has recently been proposed for the role of Nrp1 in modulating endothelial cell motility in response to VEGF (Pan et al., 2007). Neuropilin interacting protein (NIP, also known as GIPC), a PDZ domain-containing protein that interacts with the short intracellular domain of Nrps, is one such potential mediator of this process (Cai and Reed, 1999). It interacts with integrins and may modulate the signaling of many different receptor systems via its interaction with GAIP, an RGS (regulators of G protein signaling) protein (El Mourabit et al., 2002).

Nrp2 Regulates Adult Lymphangiogenesis but Is Not Required for the Maintenance of Preformed Lymphatics

Analysis of Nrp2 KO mice demonstrates that Nrp2 is a modulator of developmental lymphangiogenesis, presumably via its role as a VEGFC coreceptor (Yuan et al., 2002). However, these mutant mice form functional lymphatics after birth, suggesting that either there is compensation by another molecular mediator or the defect represents a delay rather than inhibition of lymphatic growth. The role of Nrp2 in maintaining mature lymphatics and modulating adult lymphangiogenesis is not known. Our expression analysis (Figure 4 and Figure S4) does not support a role of Nrp2 in maintaining adult lymphatics. Interestingly, Nrp2 is expressed in tumoral lymphatics and within LNs adjacent to tumors, suggesting that Nrp2 may play a role in activated or growing lymphatics. Although anti-Nrp2[B] inhibited adult lymphangiogenesis in the corneal assay, it did not have any effect on quiescent intestinal, cutaneous, pancreatic, or lymph node lymphatics, confirming that Nrp2 does not play a role in maintenance of normal lymphatics (Figure S6). Therefore, anti-Nrp2[B] treatment is unlikely to result in compromise of the normal lymphatic system leading to complications seen with use of VEGFR3 ECD, such as lymphedema (Makinen et al., 2001a).

Nrp2 Inhibition Leads to a Reduction in Functional Tumor Lymphatics and in Metastasis

Both orthotopic and subcutaneous tumor models have been extensively used to study the metastatic process, importantly, allowing modulation of early steps in the complex metastatic process (intravasation) and evaluation of the end result (distant organ metastasis). For lymphatic metastasis, subcutaneous models have the advantage of access to rich lymphatic beds and flexibility of tumor placement to allow evaluation of specific aspects of metastasis (SLN metastasis; He et al., 2002), and orthotopic models have the advantage of native microenvironment. Inhibition of the VEGFC axis, most often by the use of VEGFR3 ECD, is a commonly used strategy for reducing metastasis in both orthotopic (Chen et al., 2005) and heterotopic subcutaneous (He et al., 2002; Krishnan et al., 2003; Lin et al., 2005) settings. VEGFC may facilitate metastasis potentially by initiating lymphangiogenesis, thereby increasing the surface area of tumor cells in contact with LECs (Alitalo and Carmeliet, 2002). Given the inhibitory effect of anti-Nrp2[B] on VEGFC-induced lymphangiogenesis, we next investigated the effects of blocking Nrp2 on metastasis. To minimize confounding variables and selectively evaluate the effect of anti-Nrp2[B] on metastasis, we chose models in which blocking of Nrp2 does not affect primary tumor growth and harvested all animals at the same time point in the study. In both 66c14 and C6 tumor models, anti-Nrp2[B] treatment resulted in a significant reduction of metastatic lung nodules (Figures 5 and 6). Again, anti-Nrp2[B] treatment resulted in an equivalent block of metastasis, compared with VEGFR3 ECD, which completely blocks VEGFC signaling.

Our histologic analysis indicated that anti-Nrp2[B] did not directly affect tumor cells (data not shown). Thus, we evaluated the two potential metastatic routes available to tumor cells: blood vessels and lymphatics (Figure 7). Treatment with anti-Nrp2[B] had no effect on blood vessels but, as hypothesized on the basis of our corneal micropocket data, did reduce the density of lymphatics equivalent to that seen with VEGFR3 ECD treatment. However, these two treatments differed in the morphology and apoptotic rate of the resulting lymphatic vessels (Figure 7), further supporting a model in which Nrp2 does not simply act to augment VEGF receptor activation but also modulates VEGFC biology. Our results also demonstrate that, for the experimental paradigms tested, anti-Nrp2[B] acts to inhibit lymphangiogenesis (Figure 7). However, we cannot rule out that anti-Nrp2[B] also disrupts more established lymphatic vessels within tumors.

Because it was possible that anti-Nrp2[B] reduced total lymphatic density while sparing functional vessels (which may have different sensitivity to anti-Nrp2[B]), we evaluated the effects of blocking Nrp2 on the formation of functional lymphatic vessels. Anti-Nrp2[B] reduced the formation of functional vessels, thereby more directly linking the effects on tumor lymphatics with the observed reduction in metastasis.

Finally, to confirm the consequence of reducing functional lymphatics, we evaluated the effects of anti-Nrp2[B] on metastasis to the SLN. The SLN is the first tissue that tumor cells encounter after departing from the tumor via the lymphatics and metastasis to the SLN represents one of the earliest steps in the metastatic cascade (Stracke and Liotta, 1992). As predicted, anti-Nrp2[B] treatment resulted in a delay of the development of SLN micrometastasis, consistent with the idea that fewer cells were effluxing

from the primary tumor mass. This is consistent with evidence that VEGFC increases metastasis by inducing lymphatic hyperplasia and increased delivery of cancer cells to lymph nodes (Hoshida et al., 2006). Thus, the weight of evidence points to a mechanism by which blocking of Nrp2 leads to a reduction in functional tumor lymphatics, preventing tumor cells from initiating the metastatic process by exiting from the primary tumor mass.

EXPERIMENTAL PROCEDURES

Cell Culture and In Vitro Assays
Human dermal LECs and human umbilical vein endothelial cells (HUVECs) were purchased from Cambrex and cultured in EGM-2 medium (Cambrex). C6 LacZ cells were purchased from ATCC. 66C14 were a kind gift from F. Miller. Tumor cells were cultured in DMEM (GIBCO) supplemented with 10% FBS. All cells were maintained at 37°C in a 5% CO_2, 95% humidity incubator. Cell migration, proliferation, adhesion, and internalization (FACS) assays were performed as described elsewhere (Pan et al., 2007 and the Supplemental Data).

Animal Studies
All studies were conducted in accordance with the Guide for the Care and Use of Laboratory Animals, published by the NIH (NIH Publication 85-23, revised 1985). An Institutional Animal Care and Use Committee (IACUC) approved all animal protocols. Murine corneal micropocket assay and skin vessel permeability assay were performed as described elsewhere (Pan et al., 2007 and the Supplemental Data).

Tumor Models
66C14 (2×10^5 cells in 10 μl PBS) and C6 (2×10^6 tumor cells in 100 μl PBS) were injected into anesthetized mice as noted in the Supplemental Data. When tumors reach an average size of 80–120 mm^3, mice were sorted, to give nearly identical group mean tumor sizes, and were treated with isotype control anti-ragweed antibody (10 mg/kg), anti-Nrp2^B (10 mg/kg) or VEGFR3 ECD 25 mg/kg i.p. twice weekly until study termination. Evaluation of tumor growth and metastasis and histologic evaluation was performed as noted in the Supplemental Data.

For details on other experimental procedures, see the Supplemental Data.

SUPPLEMENTAL DATA

The Supplemental Data include Supplemental Experimental Procedures and seven supplemental figures and can be found with this article online at http://www.cancercell.org/cgi/content/full/13/4/331/DC1/.

REFERENCES

Achen, M.G., and Stacker, S.A. (2006). Tumor lymphangiogenesis and metastatic spread—New players begin to emerge. Int. J. Cancer 119, 1755–1760.

Achen, M.G., Mann, G.B., and Stacker, S.A. (2006). Targeting lymphangiogenesis to prevent tumour metastasis. Br. J. Cancer 94, 1355–1360.

Alitalo, K., and Carmeliet, P. (2002). Molecular mechanisms of lymphangiogenesis in health and disease. Cancer Cell 1, 219–227.

Aslakson, C.J., and Miller, F.R. (1992). Selective events in the metastatic process defined by analysis of the sequential dissemination of subpopulations of a mouse mammary tumor. Cancer Res. 52, 1399–1405.

Bernstein, J.J., and Woodard, C.A. (1995). Glioblastoma cells do not intravasate into blood vessels. Neurosurgery 36, 124–132.

Brkovic, A., and Sirois, M.G. (2007). Vascular permeability induced by VEGF family members in vivo: Role of endogenous PAF and NO synthesis. J. Cell. Biochem. 100, 727–737.

Cai, H., and Reed, R.R. (1999). Cloning and characterization of neuropilin-1-interacting protein: A PSD-95/Dlg/ZO-1 domain-containing protein that interacts with the cytoplasmic domain of neuropilin-1. J. Neurosci. 19, 6519–6527.

Cao, R., Eriksson, A., Kubo, H., Alitalo, K., Cao, Y., and Thyberg, J. (2004). Comparative evaluation of FGF-2-, VEGF-A-, and VEGF-C-induced angiogenesis, lymphangiogenesis, vascular fenestrations, and permeability. Circ. Res. 94, 664–670.

Carmeliet, P., and Tessier-Lavigne, M. (2005). Common mechanisms of nerve and blood vessel wiring. Nature 436, 193–200.

Chen, H., Chedotal, A., He, Z., Goodman, C.S., and Tessier-Lavigne, M. (1997). Neuropilin-2, a novel member of the neuropilin family, is a high affinity receptor for the semaphorins Sema E and Sema IV but not Sema III. Neuron 19, 547–559.

Chen, H., He, Z., Bagri, A., and Tessier-Lavigne, M. (1998). Semaphorin-neuropilin interactions underlying sympathetic axon responses to class III semaphorins. Neuron 21, 1283–1290.

Chen, Z., Varney, M.L., Backora, M.W., Cowan, K., Solheim, J.C., Talmadge, J.E., and Singh, R.K. (2005). Down-regulation of vascular endothelial cell growth factor-C expression using small interfering RNA vectors in mammary tumors inhibits tumor lymphangiogenesis and spontaneous metastasis and enhances survival. Cancer Res. 65, 9004–9011.

El Mourabit, H., Poinat, P., Koster, J., Sondermann, H., Wixler, V., Wegener, E., Laplantine, E., Geerts, D., Georges-Labouesse, E., Sonnenberg, A., et al. (2002). The PDZ domain of TIP-2/GIPC interacts with the C-terminus of the integrin α5 and α6 subunits. Matrix Biol. 21, 207–214.

Favier, B., Alam, A., Barron, P., Bonnin, J., Laboudie, P., Fons, P., Mandron, M., Herault, J.P., Neufeld, G., Savi, P., et al. (2006). Neuropilin-2 interacts with VEGFR-2 and VEGFR-3 and promotes human endothelial cell survival and migration. Blood 108, 1243–1250.

Ferrara, N., Gerber, H.P., and LeCouter, J. (2003). The biology of VEGF and its receptors. Nat. Med. 9, 669–676.

Gluzman-Poltorak, Z., Cohen, T., Herzog, Y., and Neufeld, G. (2000). Neuropilin-2 is a receptor for the vascular endothelial growth factor (VEGF) forms VEGF-145 and VEGF-165. J. Biol. Chem. 275, 29922.

Gupta, G.P., and Massague, J. (2006). Cancer metastasis: Building a framework. Cell 127, 679–695.

He, Y., Kozaki, K., Karpanen, T., Koshikawa, K., Yla-Herttuala, S., Takahashi, T., and Alitalo, K. (2002). Suppression of tumor lymphangiogenesis and lymph node metastasis by blocking vascular endothelial growth factor receptor 3 signaling. J. Natl. Cancer Inst. 94, 819–825.

Hoshida, T., Isaka, N., Hagendoorn, J., di Tomaso, E., Chen, Y.-L., Pytowski, B., Fukumura, D., Padera, T.P., and Jain, R.K. (2006). Imaging steps of lymphatic metastasis reveals that vascular endothelial growth factor-c increases metastasis by increasing delivery of cancer cells to lymph nodes: Therapeutic implications. Cancer Res. 66, 8065–8075.

Isaka, N., Padera, T., Fukumura, D., and Jain, R.K. (2004). Peritumor lymphatics induced by VEGF-C exhibit abnormal function. Cancer Res. 64, 4400–4404.

Ji, R.C., and Kato, S. (2003). Lymphatic network and lymphangiogenesis in the gastric wall. J. Histochem. Cytochem. 51, 331–338.

Joukov, V., Sorsa, T., Kumar, V., Jeltsch, M., Claesson-Welsh, L., Cao, Y., Saksela, O., Kalkkinen, N., and Alitalo, K. (1997). Proteolytic processing regulates receptor specificity and activity of VEGF-C. EMBO J. 16, 3898–3911.

Joukov, V., Kumar, V., Sorsa, T., Arighi, E., Weich, H., Saksela, O., and Alitalo, K. (1998). A recombinant mutant vascular endothelial growth factor-C that has

lost vascular endothelial growth factor receptor-2 binding, activation, and vascular permeability activities. J. Biol. Chem. *273*, 6599–6602.

Karpanen, T., Heckman, C.A., Keskitalo, S., Jeltsch, M., Ollila, H., Neufeld, G., Tamagnone, L., and Alitalo, K. (2006). Functional interaction of VEGF-C and VEGF-D with neuropilin receptors. FASEB J. *20*, 1462–1472.

Krishnan, J., Kirkin, V., Steffen, A., Hegen, M., Weih, D., Tomarev, S., Wilting, J., and Sleeman, J.P. (2003). Differential in vivo and in vitro expression of vascular endothelial growth factor (VEGF)-C and VEGF-D in tumors and its relationship to lymphatic metastasis in immunocompetent rats. Cancer Res. *63*, 713–722.

Kubo, H., Cao, R., Brakenhielm, E., Makinen, T., Cao, Y., and Alitalo, K. (2002). Blockade of vascular endothelial growth factor receptor-3 signaling inhibits fibroblast growth factor-2-induced lymphangiogenesis in mouse cornea. Proc. Natl. Acad. Sci. USA *99*, 8868–8873.

Li, X.F., Zanzonico, P., Ling, C.C., and O'Donoghue, J. (2006). Visualization of experimental lung and bone metastases in live nude mice by X-ray micro-computed tomography. Technol. Cancer Res. Treat. *5*, 147–155.

Lin, J., Lalani, A.S., Harding, T.C., Gonzalez, M., Wu, W.W., Luan, B., Tu, G.H., Koprivnikar, K., VanRoey, M.J., He, Y., et al. (2005). Inhibition of lymphogenous metastasis using adeno-associated virus-mediated gene transfer of a soluble VEGFR-3 decoy receptor. Cancer Res. *65*, 6901–6909.

Makinen, T., Jussila, L., Veikkola, T., Karpanen, T., Kettunen, M.I., Pulkkanen, K.J., Kauppinen, R., Jackson, D.G., Kubo, H., Nishikawa, S., et al. (2001a). Inhibition of lymphangiogenesis with resulting lymphedema in transgenic mice expressing soluble VEGF receptor-3. Nat. Med. *7*, 199–205.

Makinen, T., Veikkola, T., Mustjoki, S., Karpanen, T., Catimel, B., Nice, E.C., Wise, L., Mercer, A., Kowalski, H., Kerjaschki, D., et al. (2001b). Isolated lymphatic endothelial cells transduce growth, survival and migratory signals via the VEGF-C/D receptor VEGFR-3. EMBO J. *20*, 4762–4773.

Nathanson, S.D. (2003). Insights into the mechanisms of lymph node metastasis. Cancer *98*, 413–423.

Padera, T.P., Kadambi, A., di Tomaso, E., Carreira, C.M., Brown, E.B., Boucher, Y., Choi, N.C., Mathisen, D., Wain, J., Mark, E.J., et al. (2002). Lymphatic metastasis in the absence of functional intratumor lymphatics. Science *296*, 1883–1886.

Pan, Q., Chanthery, Y., Liang, W.C., Stawicki, S., Mak, J., Rathore, N., Tong, R.K., Kowalski, J., Yee, S.F., Pacheco, G., et al. (2007). Blocking neuropilin-1 function has an additive effect with anti-VEGF to inhibit tumor growth. Cancer Cell *11*, 53–67.

Soker, S., Miao, H.Q., Nomi, M., Takashima, S., and Klagsbrun, M. (2002). VEGF mediates formation of complexes containing VEGFR-2 and neuropilin-1 that enhance VEGF-receptor binding. J. Cell. Biochem. *85*, 357–368.

Stacker, S.A., Achen, M.G., Jussila, L., Baldwin, M.E., and Alitalo, K. (2002a). Lymphangiogenesis and cancer metastasis. Nat. Rev. Cancer *2*, 573–583.

Stacker, S.A., Baldwin, M.E., and Achen, M.G. (2002b). The role of tumor lymphangiogenesis in metastatic spread. FASEB J. *16*, 922–934.

Stracke, M.L., and Liotta, L.A. (1992). Multi-step cascade of tumor cell metastasis. In Vivo *6*, 309–316.

Wang, L., Zeng, H., Wang, P., Soker, S., and Mukhopadhyay, D. (2003). Neuropilin-1-mediated vascular permeability factor/vascular endothelial growth factor-dependent endothelial cell migration. J. Biol. Chem. *278*, 48848–48860.

Yuan, L., Moyon, D., Pardanaud, L., Breant, C., Karkkainen, M.J., Alitalo, K., and Eichmann, A. (2002). Abnormal lymphatic vessel development in neuropilin 2 mutant mice. Development *129*, 4797–4806.